

Spectrum of recoil nucleons in quasi-elastic neutrino-nucleus interactions

Cezary Juszczak, Jarosław A. Nowak, Jan T. Sobczyk^{*a}

^aInstitute of Theoretical Physics, Wrocław University.
pl. M. Borna 9, 50-204 Wrocław, Poland

We have analyzed the consequences of introducing the local density approximation combined with an effective nuclear momentum-dependent potential into the CC quasi-elastic neutrino-nucleus scattering. We note that the distribution of the recoil nucleons momenta becomes smooth for low momentum values and the sharp threshold is removed. Our results may be relevant for Sci-Fi detector analysis of K2K experiments. The total amount of observed recoil protons is reduced because some of them remain bound inside the nucleus. We compare theoretical predictions for a probability of such events with the results given by NUX+FLUKA MC simulations.

1. INTRODUCTION

In recent years there has been growing interest in the studies of neutrino interactions at energies of a few GeV [1]. It was motivated by the need for more precise measurements of neutrino oscillation parameters (θ_{13} in particular). This entails deriving the best description of interactions with free nucleons, and then incorporating nuclear effects. From the point of view of the Monte Carlo codes most (or all) nuclear effects are described with numerical packages [2] but it is enlightening how many of these effects can be presented in an analytical form.

We investigated the process $\nu_\mu n \rightarrow \mu^- p$ with the target neutron bound inside the nucleus. Computations of nuclear effects were based on the Fermi gas model which is known to work well in the above mentioned energy region [3]. But this approach is not completely satisfactory. For example its simple form leads to the conclusion that the ejected nucleons can only have momenta higher than the chosen value of the Fermi momentum k_F [4]. However there seems to be no physical reason why lower values of momenta should be forbidden.

A possible solution to this problem is to introduce a local density approximation [5]. In fact the density of nuclear matter is not uniform and ac-

cordingly it is possible to introduce the concept of local Fermi momentum $k_F(r)$. Since the interaction can take place in a region where Fermi momentum is arbitrarily low, the distribution of momenta of recoil nucleons becomes smoother.

Another solution can be based on a different effect. The target nucleons are not free but they are bound inside the nucleus. The binding energy is smaller than the typical values of energy transfer but it may cause interesting effects. Momentum dependent optical potential can be obtained even from the simplest versions of nuclear mean field theory [6]. In the covariant approach based on the Dirac equation one has to distinguish contributions from scalar and vector components of nucleon self-energy in nuclear matter. In this framework the electron-nuclei scattering was discussed in [7] with mean fields taken from [8]. More recent results on the self-energy can be found e.g. in [9] where derivations used the G-matrix approach. Our investigation is based on other computations [10]. This choice was dictated by two reasons. Firstly we were able to reproduce an explicit formula for the potential as a function of density (local Fermi momentum) and nucleon momentum. Secondly we wanted to enable comparisons with the numerical results of other authors who used the same potential [11].

We wanted to describe both local density and potential effects and for that we needed an analytical form of the potential. So we have derived a simple analytical form of the potential depen-

^{*}J.T. Sobczyk was supported by KBN grant 105/E-344/SPB/ICARUS/P-03/DZ211/2003-2005; C. Juszczak and J.A. Nowak were supported by LNGS-TARI P10/02

dent on two variables: the Fermi momentum and the nucleon momentum. We incorporated this potential into a Monte Carlo generator of events and obtained a spectrum of the ejected nucleon momentum. The simulations were performed for three target nuclei: oxygen, iron and argon; these are possible targets in the neutrino experiments. The results in all three cases were very similar because the shapes and the density profiles did not differ significantly.

We investigated also the possibility that the effective potential leads to reduction of the number of the produced protons that escape from the nucleus. We compute the fraction of the total cross section which can be interpreted as corresponding to an excited nucleus in the final state. The same effect is predicted by other MC generators e.g. by NUX+FLUKA.

We have also looked for the effects related to the proton-neutron asymmetry inside the nucleus. It turned out that the introduction of separate values of the Fermi momentum for proton and neutron gases left all the plots virtually unchanged.

Our results can be useful in near detector analysis of neutrino interaction events in K2K where Sci-Fi detector registers tracks of ejected protons. The reconstruction procedure requires the particle to cross at least 3 planes of scintillating fiber thus the protons would need a momentum greater than 500 MeV. Therefore in the data analysis it is important to have MC which correctly describes the shape of the distribution of recoil protons momenta.

We performed MC simulations assuming the neutrino energy profile expected at Sci-Fi detector [12]. We investigated to what extent the spectrum of the recoil proton momentum is influenced by the introduction of the LDA and the effective potential.

We restricted ourselves to a simplified dynamic model without the effects caused by the RPA correlations. We also excluded from our analysis the effects due to the final state interactions in nuclei.

The spectrum of the ejected nucleon momentum was studied earlier in the context of NC reactions where it is the only observable quantity. The outgoing nucleons with higher momentum

(above the Cherenkov threshold for SK i.e. bigger than about 1.07 GeV) were studied recently in [13]. In an earlier study [14] an average binding energy was used to describe kinematics of the process and interesting predictions for angular distributions of recoil nucleons were proposed. Pauli blocking was not imposed and arbitrarily low values of the momenta of ejected nucleons were obtained. Another approach [15] used Pauli blocking and forbade recoil nucleons of kinetic energy lower than about 27 MeV. It seems clear that any realistic model of interaction should incorporate Pauli blocking and consequently also a mechanism to remove the nonphysical threshold in the ejected nucleon momentum spectrum.

2. MODEL

Our Monte Carlo generator simulates quasi-elastic neutrino interactions with basic dynamics introduced according to [16].

The events are obtained in the following manner:

- The neutrino energy E_ν is chosen as either a fixed value or generated according to some beam energy profile.
- The Fermi momentum is established using global or local Fermi momentum scheme:
 - In the global scheme the Fermi momentum is fixed.
 - In the local scheme the region in the nucleon where the interaction is going to take place is selected first. Then the Fermi momentum is calculated based on the nuclear density in this region.

The actual target momentum is chosen at random from the Fermi ball of that radius.

- The nucleon neutrino pair is boosted to its center of mass frame (CMS) where the direction of the scattering is taken to be random but it will be weighted later on.
- While keeping this direction fixed in the CMS frame various values of the outgoing nucleon momentum are tested and by

means of the bisection algorithm the value which brings about the energy conservation is chosen. The energy is always evaluated in the LAB frame and takes in the account the momentum dependent potential of the nucleon.

- The outgoing nucleon is Pauli blocked if its momentum in the lab is smaller than the local fermi momentum.
- The exit of the nucleon from the nuclear matter is simulated by diminishing the values of its momentum from the above calculated value p_N (inside nucleus) to the value p' (outside nucleus) calculated from the energy conservation condition

$$V(p_N) + E_k(p_N) = E_k(p') \quad (1)$$

If there is no solution then the proton is unable to leave the nucleus and the nucleus becomes excited. The justification for this equation comes from the fact that there is no nuclear potential outside the nucleus.

- The value of cross section is calculated according to neutrino energy in the target rest frame. A correction of little significance (less than 1 % effect on the cross section) due to nonlinearity of the neutrino and target nucleon momenta is taken into account. The weight of the event is proportional to the nuclear density, differential cross section (with correction), the boost jacobian, the bisection algorithm jacobian.

The target is treated as a collection of nucleons distributed in space according to the density profile determined by electron-nucleus scattering experiments. For ${}^{16}_8\text{O}$ we adopted the harmonic oscillator model in which the nuclear density is given by [17]:

$$\rho^{16\text{O}}(r) = \rho_0 \exp(-r^2/R^2) \left(1 + C \frac{r^2}{R^2}\right) \quad (2)$$

where $R = 1.883 \text{ fm}$, $\rho_0 = 0.141 \text{ fm}^{-3}$, $C = 1.544$, and ρ_0 is a normalization constant defined by the condition:

$$\int d^3r \rho^{16\text{O}}(r) = A. \quad (3)$$

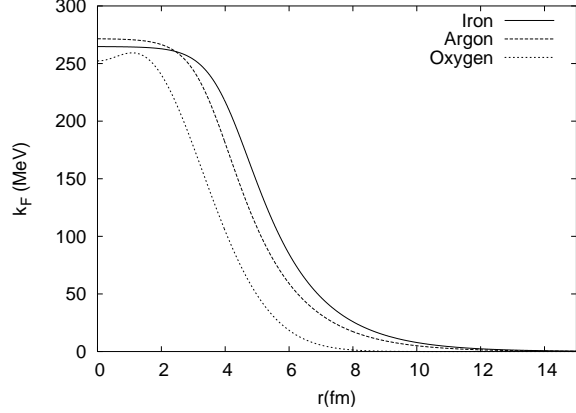


Figure 1. The local Fermi momentum r dependence for ${}^{16}_8\text{O}$, ${}^{40}_{18}\text{Ar}$ and ${}^{56}_{26}\text{Fe}$.

For ${}^{40}_{18}\text{Ar}$ and ${}^{56}_{26}\text{Fe}$ we use the two parameter Fermi model and write the density as:

$$\rho^{Ar, Fe}(r) = \frac{\rho_0}{1 + \exp\left(\frac{r-C}{C_1}\right)} \quad (4)$$

with the following parameters:

	$\rho_0[\text{fm}^{-3}]$	$C[\text{fm}]$	$C_1[\text{fm}]$
${}^{40}_{18}\text{Ar}$	0.176	3.530	0.541
${}^{56}_{26}\text{Fe}$	0.163	4.111	0.558

The local Fermi momentum is determined by the density profile according to:

$$k_F(r) = \sqrt[3]{\frac{3\pi^2\rho(r)}{2}} \quad (5)$$

In fig. 1 we show the local Fermi momentum dependence on r for Oxygen, Argon and Iron. In the case of nonsymmetric nuclei one can also introduce separate local Fermi momenta for protons and neutrons:

$$k_F^p(r) = \sqrt[3]{\frac{2Z}{A}} k_F(r), \quad k_F^n(r) = \sqrt[3]{\frac{2N}{A}} k_F(r). \quad (6)$$

where A , Z , and N are the atomic number, the number of protons, and the number of neutrons in the nucleus respectively.

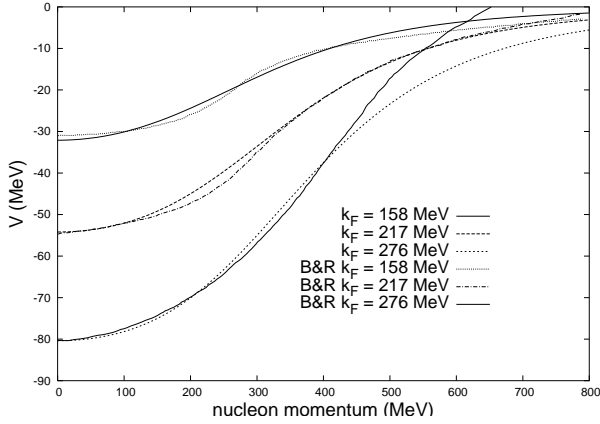


Figure 2. Momentum dependent potential $V(k_F, p)$ for 3 values of Fermi momentum (see formula (7)) compared with three original plots taken from [11].

The average value of k_F is calculated as:

$$\langle k_F^{nucleus} \rangle = \frac{\int k_F(r) r^2 \rho^{nucleus}(r) dr}{\int r^2 \rho^{nucleus}(r) dr}. \quad (7)$$

We get the following values:

$$\begin{aligned} \langle k_F^O \rangle &= 199 \text{ MeV}, \\ \langle k_F^{Ar} \rangle &= 217 \text{ MeV}, \\ \langle k_F^{Fe} \rangle &= 217 \text{ MeV}. \end{aligned}$$

Using results from [10] we find an analytic form of the real part of the optical potential as (see fig. 2):

$$V(k_F, p) = -\frac{(ak_F)^2 (k_F + b)}{c^4 + d^3 k_f + e^3 p^2 / k_f + p^4}, \quad (8)$$

where k_F , p , and $V(k_F, p)$ are given in MeV. The fitted values of the parameters are: $a = 206 \text{ MeV}$, $b = 582 \text{ MeV}$, $c = -322 \text{ MeV}$, $d = 422 \text{ MeV}$, and $e = 289 \text{ MeV}$.

The formula (8) fulfills the following criteria:

- V is negative

- V reproduces essential features of plots from [10],
- V is monotonously increasing,
- For higher values of momentum, V quickly approaches zero,
- For small values of momentum, V is proportional to p^2 as in the limit as $p \rightarrow 0$ on general ground one expects that

$$V(p) \sim V_0 + \frac{p^2}{2M^*} \quad (9)$$

There is some amount of uncertainty in the reconstructed potential which is inherited from the original computations in which contributions from only finite number of harmonics were included.

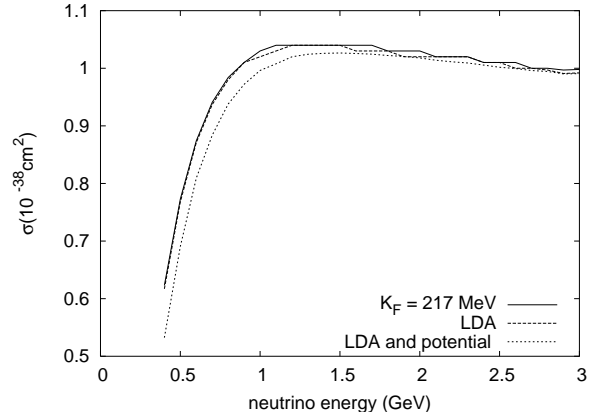


Figure 3. Total cross section for quasi-elastic scattering on iron nucleus per nucleon.

In numerical computations we compare three cases:

- Fermi gas with global $k_F = \langle k_F^{nucleus} \rangle$,
- Fermi gas in local density approximation (LDA),

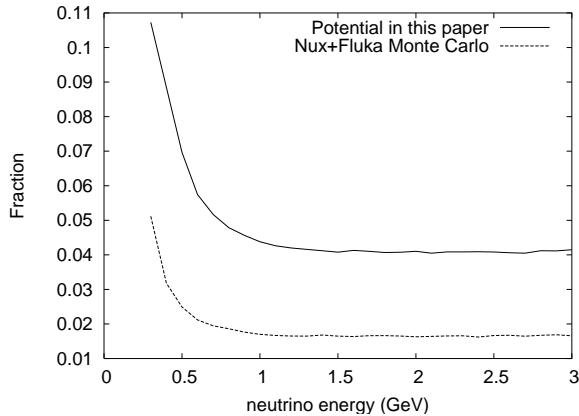


Figure 4. A fraction of the total cross section corresponding to events in which proton remains bounded in excited nucleus.

- (c) Fermi gas with in the local density approximation with momentum dependent nucleon potential (8).

3. RESULTS

The total cross sections for quasi-elastic interaction for all three cases are plotted in fig. 3. While changes introduced by the LDA are minor, the effective potential reduces the total cross section by a few percent. Since the produced proton is affected by momentum depended potential it may not have enough energy to leave the nucleus. In such a case in the final state the nucleus is excited and there is no ejected nucleon. This happens always if

$$V(p_N) + E_k(p_N) \leq M. \quad (10)$$

The probability of such a process is shown in fig. 4. For comparison we calculated the probability of analogous events in the NUX+FLUKA MC generator. It is very interesting that the shapes of the curves are in both cases almost identical. The probability for a bound nucleon in the final state decreases with neutrino energy in both generators and at energy of about 1 GeV becomes flat.

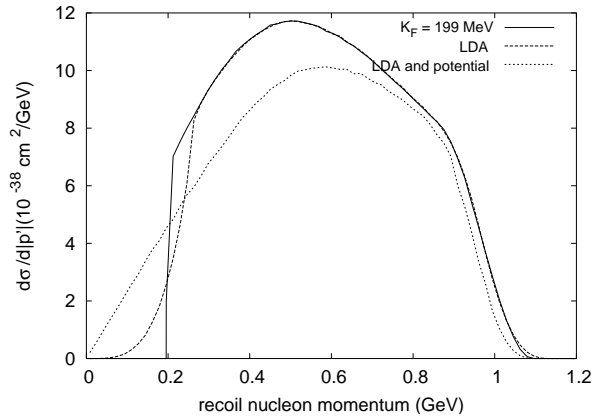


Figure 5. Quasielastic neutrino-oxygen scattering: recoil nucleons momentum distribution at $E_\nu = 700$ MeV.

However, the effect predicted by our Monte Carlo generator is much bigger (about three times).

The predicted distributions of the ejected nucleon momentum are shown in fig. 5 and 6. The plots are normalized as differential cross sections $d\sigma/dp'$. In all cases the neutrino energy is fixed at $E_\nu = 700$ MeV. The changes observed due to the LDA and the effective potential are very similar for all three analyzed targets so we do not include a plot for iron.

In the case (a) there are obvious sharp thresholds at $\langle k_F^{nucleus} \rangle$.

In the case (b) the distributions become smoother. They differ only in the region of nucleon momentum below ~ 300 MeV; whereas, for higher values of nuclear momentum, LDA introduces no significant differences.

Finally, in the case (c) there is higher probability for the outgoing nucleon to have momentum lower than k_F . The values close to zero become accessible as well. The differential cross section rises almost linearly for nucleon momenta smaller than 450 MeV then it slowly bends reaching maximum at about 600 MeV. For momenta above 800 MeV the plot is only slightly changed com-

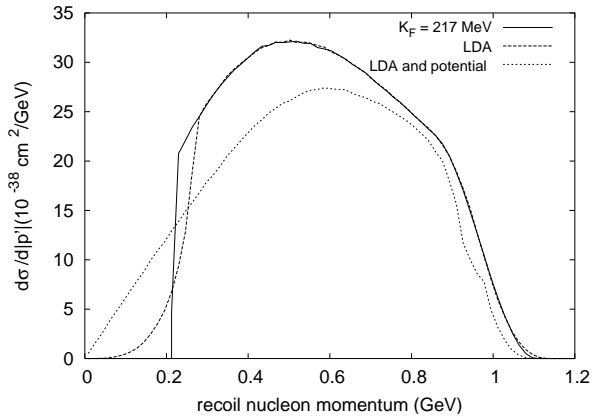


Figure 6. Quasielastic neutrino-argon scattering: recoil nucleons momentum distribution at $E_\nu = 700$ MeV.

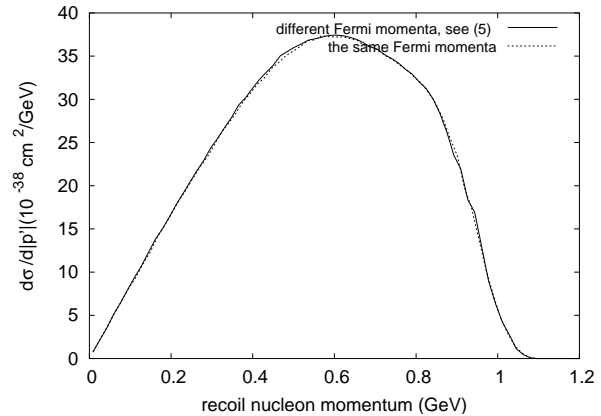


Figure 7. Effect of different Fermi momenta for proton and neutron Fermi gases in quasielastic neutrino-iron scattering for ejected momentum distribution at $E_\nu = 700$ MeV.

pared to the cases (a) and (b).

The fig. 7 illustrates the relevance of the introduction of separate values of Fermi momentum for neutron and proton Fermi gases. The Fermi momentum for neutrons is larger and since the interaction takes place on neutrons, it is clear that the cross section should be slightly larger. It is indeed the case but the effect is very small and the difference of the plots is hardly noticeable.

For completeness in fig. 8 we present how both discussed effects influence the energy transfer spectrum for the iron nucleus (plots for oxygen and argon are very similar). There is only a small difference at the peak between the differential cross section plots for the cases (a) and (b) the plot for the LDA being slightly lower. In the case (c) we observe a significant change in the shape of the plot. For lower values of the energy transfer the differential cross section is substantially reduced and for higher energy transfers it is slightly increased. The allowed kinematical region is also modified.

In fig. 9 we show the ejected proton momentum distribution obtained for neutrino beam with the energy profile identical to that predicted for the

K2K near detector. We note that the LDA and the potential effects remove the sharp threshold and give a smooth plot at low values of the momentum. The number of nucleons with momentum between k_F and 700 MeV is significantly reduced but the values between 0 and k_F become possible.

In fig. 10 we show the energy transfer distribution for quasi-elastic events produced with the same K2K-like beam. It is clear that it is insensitive to the effects discussed in the present paper.

REFERENCES

1. J.G. Morfin, M. Sakuda, Y. Suzuki (eds) Proceedings of the First International Workshop on Neutrino-Nucleus Interactions in the Few GeV Region, Nucl. Phys. B (Proc. Suppl.) **112** (2002) NOVEMBER 2002; for talks on NuInt02 Workshops see <http://nuint.ps.uci.edu/>
2. G. Battistoni, A. Ferrari, A. Rubbia and P.R. Sala, *The FLUKA nuclear cascade model applied to neutrino interactions*, to

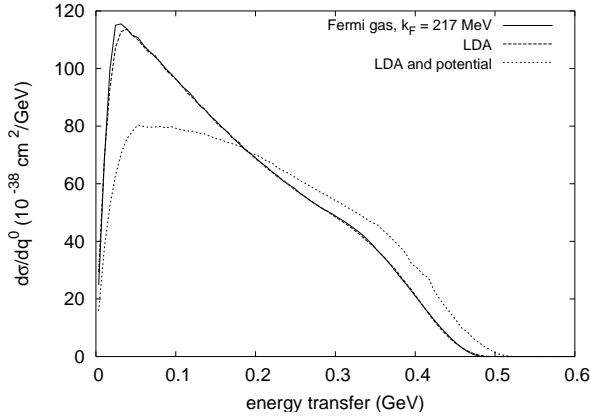


Figure 8. Differential cross section of energy transfer for quasielastic neutrino scattering on Iron; $E_\nu = 700\text{MeV}$.

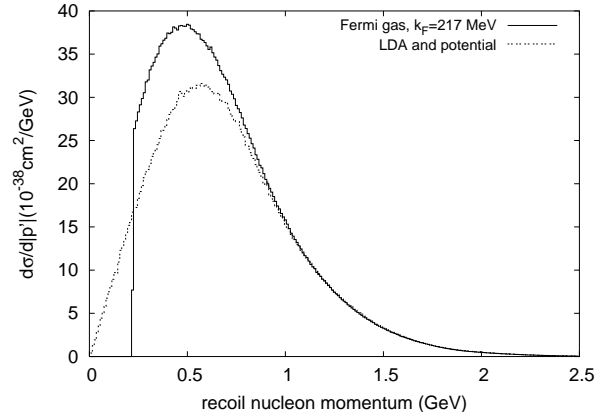


Figure 9. Distribution of recoil nucleons from quasi-elastic reactions on iron for neutrino energy spectrum identical with that of K2K at near detector. The plot is normalized to be an effective (energy averaged) differential cross section of ejected nucleon momentum. LDA and potential effects reduce the total cross section and there is also a probability of about 4% that the proton does not leave nucleus. In effect the area below the corresponding curve is reduced.

- appear in Proc. of NUINT 2002; see <http://nuint.ps.uci.edu/>
3. R.A. Smith, E.J. Moniz, Nucl. Phys. **B43** (1972) 605.
 4. C.W. Walter for the K2K Sci-Fi group, *Quasi-Elastic Events and Nuclear Effects with the K2K Sci-Fi Detector*, Nucl. Phys. B (Proc. Suppl.) **112** (2002) 140.
 5. S.K. Singh, E. Oset, Phys. Rev. C **48** (1993) 1246; T.S. Kosmas, E. Oset, Phys. Rev. C **53** (1996) 1409.
 6. B.D. Serot, J.D. Walecka, Adv. Nucl. Phys. **16** (1986) 1.
 7. H. Kim, C.J. Horowitz, M.R. Frank, Phys. Rev. C **51** (1995) 792.
 8. E.D. Cooper, S. Hama, B.C. Clark, R.L. Mercer, Phys. Rev. C **47** (1993) 297.
 9. E. Schiller, H. M  ther, Eur. Phys. J. A **11** (2001) 15.
 10. F.A. Brieva and J.R. Rook, Nuclear Physics **A291** (1977) 299.
 11. F.A. Brieva, A. Dellafore, Nucl. Phys. A **292** (1977) 445; H. Nakamura, R. Seki, *Quasi-elastic Neutrino-Nucleus Scattering and Spectral Function*, Nucl. Phys. B (Proc. Suppl.)

- 112** (2002) 197.
12. S. H. Ahn, et al (K2K collaboration), *Detection of Accelerator-Produced Neutrinos at a Distance of 250 km*, Phys.Lett. **B511** (2001) 178.
13. J.F. Beacom, S.Palomares-Ruiz, Phys. Rev. **D67** (2003) 093001.
14. C.J. Horowitz, H. Kim, D.P. Murdock, S. Pollock, Phys. Rev. C **48** (1993) 3078.
15. W.M. Alberico et al, Nucl. Phys. A **623** (1997) 471.
16. C.H. Llewellyn Smith, Phys. Rep **3**, no 5 (1972) 261.
17. H. De Vries, C.W de Jager, and C. De Vries *Atomic Data and Nuclear Tables* **36**, (1987)495

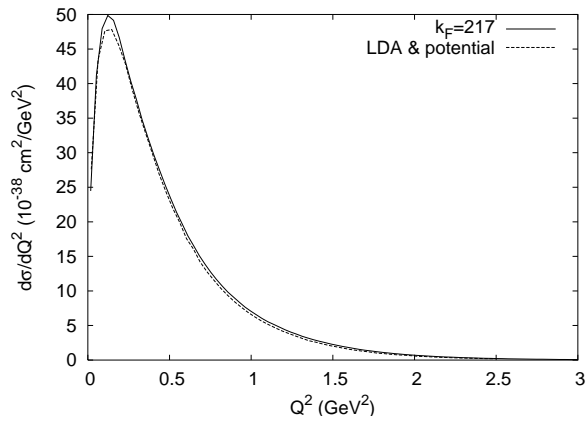


Figure 10. Differential cross section of Q^2 transfer for quasi-elastic reaction on iron with K2K neutrino beam.